

## Magnetic Resonance Imaging of the One-Humped Camel (*Camelus Dromedarius*) Digits

El-Shafey, A.A.<sup>1</sup> and Abd Al-Galil, A.S.A.<sup>2</sup>.

<sup>1</sup>Dept. Anat. & Embry, Fac. Vet. Med., Benha Univ. Egypt.

<sup>2</sup>Dept. Surgery, Anesthesiology and Radiology, Fac. Vet. Med. Benha Univ., Egypt.

[Elshafey74@yahoo.com](mailto:Elshafey74@yahoo.com) [Atef\\_abdalgalil2005@yahoo.com](mailto:Atef_abdalgalil2005@yahoo.com)

**Abstract:** The present study aimed to describe the normal anatomical structures of the digits and footpad of the camel using Magnetic Resonance Image (MRI) as well as to provide an atlas of synchronized normal Magnetic Resonance Image (MRI) and cross sectional anatomy of the digits in the camel. Sagittal, Dorsopalmar and Transverse MRI images of three isolated camel cadaver digits were obtained using "Hitachi T2-NT a magnet of 0.2 Tesla and T1 Weighted sequence". The MRI images were compared to corresponding dissect specimens and frozen cross-sections of the cadaver digits. Clinically relevant anatomic structures were identified and labeled at each level in the corresponding images (MRI and anatomic slices). The MRI images provided anatomical detail of the digits and foot of the camel. Transversal images provided excellent depiction of anatomical structures when compared to corresponding frozen cross-sections. MRI images of the current study would serve as an initial reference for normal anatomy and clinical imaging studies of the camel digits and foot that can be used by radiologist, clinicians, surgeons or for research propose in camel lameness.

[El-Shafey, A.A and Abd Al-Galil, A.S.A. **Magnetic Resonance Imaging of the One-Humped Camel (*Camelus Dromedarius*) Digits.** *J Am Sci* 2012;8(9):549-556]. (ISSN: 1545-1003). <http://www.jofamericanscience.org>. 75

**Keywords:** Magnetic resonance image. Camel. Digits.

### 1. Introduction

Camel is a unique among artiodactyls in their regular employment of pacing gait and having a unique foot morphology assumed to be an adaptation for this mode of locomotion (Webb, 1972 and Janis, *et al.*, 2002). The uniquely designed wide spread feet enable him to walk on shifting sand in the desert and rough rocky terrain whereas the footpad is used to grip onto rock and steep inclines. Their feet are secondarily digitigrades, with a splayed -toed foot, loss of hooves, addition of a broad foot pad and loss of the interdigital ligaments, allowing the divergence of the third and fourth digits, (Janis, *et al.*, 2002 and Masahiko *et al.*, 2002).

The diseases of the metacarpus and digits are not rare, which necessitates awareness with its normal structure to be able to recognize changes in the diseased animal. Classical anatomic atlases cannot provide the spectrum of views and the details required in modern diagnostic and surgical techniques (Gehrmann *et al.*, 2006; Dyson and Murray, 2007; Raji *et al.*, 2008 and Vanderperren *et al.*, 2008).

The camel digits and feet are differ from those of other domestic animals and have a complex structure with tendons, joints and ligaments (Smuta and Bezuidenhout, 1987 and Nickle, *et al.*, 1995). Few studies had been done on the camel digits by the current diagnostic imaging techniques such as Radiography and ultrasonography which provide limited information for evaluation of the camel digits and feet (Fahmy, *et al.*, 2002). Radiography has limited value to evaluation of soft tissue, although ultrasonography

provides visualization of the tendons and ligaments (Kazer-hotz *et al.*, 1994, Lisher, and Walliser, 2005), however, ultrasonography provides a small field of view and each structure has to be imaged separately, and a cross sectional examination through the entire digit is not possible. On the other hand, soft tissue is difficult to be evaluated by ultrasonography in the digit (Denoux *et al.*, 1993).

Computed tomography (CT) and Magnetic resonance imaging currently plays a prominent role in the diagnosis and evaluation of many human diseases (Goncalves-Fetreira *et al.*, 2001). It was not initially used in veterinary medicine because of its limited accessibility and high costs. However accessibility has improved, which has increased the need of expertise in the use of this technique in animals (Kazer-hotz *et al.*, 1994; Ottesen and Moel, 1998 ; Bienert and Stadler, 2006, Bahgat, 2007 and Raji *et al.*, 2009).

Since MRI have become more available to veterinarians, the knowledge of the normal conventional anatomy and radiographic anatomy could no longer serve as a basis for recognizing structural abnormalities in diseased animals (Kraft *et al.*, 1986; Kakhainen *et al.*, 1991; Morgan *et al.*, 1993; Hundson *et al.*, 1995 and Assheuer and Sager, 1997).

The use of MRI in large animal medicine is currently limited by logistical problems of acquiring MRI images; meanwhile a few MRI studies on horses' digit have been done for example (Kleitoeer *et al.*, 1999; Hevesi *et al.*, 2004 and Murray *et al.*, 2004) and on bovine' digits (Raji *et al.*, 2009).

MR imaging of the equine distal limb has revealed multiple bone abnormalities that are not visible with radiography. MR is able to distinguish pathologic changes occurring at the molecular level. This enables visualization of inflammatory fluid within bone that cannot be visualized radiographically. Lesions that produce inflammatory fluid within the bone include bone bruises, microfractures, and injuries at the origin and insertions of ligaments and tendons (Zubrod *et al.*, 2004; Sampson *et al.*, 2005 and Sampson and Tucker, 2007).

The present work was carried out to provide a reference of synchronized normal MRI and gross anatomic sections of the digits of the camel, to outstand a basis for diagnosis of their diseases by the aid of MRI.

## 2. Material and methods

The present work was carried out on the digits of nine healthy asymptomatic adult camels of 10-15 years old. The specimens were obtained from Tokh slaughter house immediately after slaughter, by disarticulating the carpometacarpal joints, cooled and imaged within 12 hours to minimize post-mortem changes.

The specimens underwent consecutive MRI scan, which performed at the Imaging Diagnostic Center, Habeb MRI center, by using "Hitachi T2-NT a magnet of 0.2 Tesla and T1 Weighted sequence" by a standard human body coil". Continuous series of Sagittal, Dorsopalmar and Transverse scan were obtained from the digits. T1- Weighted MRI images were acquired using the following parameters: repetition time ( $T_R$ ) = 630MS, echo time ( $T_E$ ) = 18 ms. 5mm slice thickness with 1mm inter slice spacing.

After MRI images were obtained, the camel digits were frozen at  $-20^\circ$  then the digits sectioned in sagittal, dorsopalmar and transverse planes in 1-cm slices using an electric band saw, to correspond with the MRI images. All sections were cleaned, photographed, the frozen sectioned were fixed in 10% formalin for further anatomic dissection.

Important anatomic structures were detected and labeled in gross sections photographs and its corresponding MRI scans. The cross-sections were exposed in a proximal to distal progression from the level of metacarpophalangeal joint to 1cm distal to the coffin joint. The nomenclature used in this work was adapted to Schaller, 2007 and the Nomina Anatomica Veterinaria, (2005).

## 3. Results

The results of the present study were performed on 8 MRI images of the camel four digits. 8 gross sections photographs most closely corresponding with MRI images were selected as follows, sagittal (Fig.1), dorsopalmar (Fig. 2), and transverse (Figs. 3 - 8). The transversal MRI images were selected at levels of

Metacarpophalangeal joint, proximal extremity of proximal phalanx, middle of the body (shaft) of the proximal phalanx, distal extremity of proximal phalanx, proximal interphalangeal (pastern) joint and distal interphalangeal (Coffin) joint. MRI provided good discrimination between bone and soft tissue and moderate discrimination between the adjacent soft tissues according to their physical density difference. The transversal MRI images provided excellent depictions of anatomical structures when compared to their corresponding gross sections photographs. Identifiable anatomic structure was labeled on the line drawings of the limb sections and on the corresponding MRI images.

MRI images provide excellent anatomic depiction of the camel digits as it provided excellent discrimination between bone and soft tissue and good discrimination between the adjacent soft tissues according to their physical density difference.

In MRI images, cortex of phalanx, fat, skin and hoof were observed and had intermediate signal intensity and appeared grey (Figs. 1,2).

Tendons, blood vessels, synovial cavity and corium of hoof had a hyperintense signal and appeared black (Fig. 2).

Medulla of phalanx had low signal intensity and appeared white (Fig.1). Proximal, middle and distal phalanx, proximal sesamoid bones, distal sesamoid cartilage (navicular cartilage), nail, superficial digital flexor tendon (SDF), deep digital flexor tendon (DDF), interosseous muscle, , navicular bursa and common dorsal digital artery were clearly identify in MRI images (Figs. 1-5).

Two metacarpophalangeal (fetlock) joints (Fig. 3), were present in each fore limb, one for each digit. The articular cavity (Fig. 3a/7) was a potential cavity so it did not appear in the MRI images, while in the cross sectional anatomy, it appeared linear, except it was widened artificially (Fig. 3b/7). The axial and abaxial proximal sesamoid bones of each metacarpophalangeal joint were connected by a palmar ligament (Fig. 3/9 ). Each abaxial proximal sesamoid bone was attached to the corresponding (medial or lateral) aspect of the distal extremity of the fused third and fourth metacarpal bones by a collateral sesamoideum ligament (Fig. 3/8).

The interdigital ligament (Fig. 7/6) connects the third and fourth digits at the level of the middle interphalangeal joint and continuous to the level of the coffin joint.

The tendon of M. extensor digitorum lateralis (Fig. 3/3& 4/3) on the dorsum of the proximal and middle phalanges of the 4<sup>th</sup> digit, and the tendon of the of M. extensor digitorum communis (Fig. 3/4, 4/4, 5/3 & 6/3) on the dorsum of the proximal and middle phalanges of the third digit, were differentiated in the cross sectional anatomy when the intervening Fascia

dorsalis manus was dissected to demonstrate these tendons. These structures appeared in the MRI images as a narrow transverse strap on the dorsum of the proximal and middle phalanges.

On the palmar aspect of the digits, the cross sectional anatomy differentiated the tendon of the deep digital flexor tendon (Figs. 3/10, 4/8, 5/5, 6/5& 7/5) and superficial digital flexor tendon (Figs. 3/11, 4/7, 5/4, 6/4, 7/4), only when the fascia palmaris was dissected to demonstrate these tendons. These structures appeared in the MRI images as a rounded gray mass and their outlines were differentiated.

The superficial digital flexor tendon gained a position deeper to that of the deep digital flexor tendon,

just distal to the fetlock joint, and prior to its insertion in the proximal end of the middle phalanx, (Figs. 1, 5 & 6).

The proximal interdigital (pastern joint) (Fig. 7) was formed by articulation of the distal end of the proximal phalanx and the proximal end of the middle phalanx.

The distal interphalangeal (coffin) joint (Fig. 8) is the formed by articulation of the distal end of the middle phalanx, the distal phalanx and the distal sesamoid (navicular) cartilage ((Fig. 1/12). The articular cavity ((Fig. 8/5) was a potential cavity so it appeared linear in the cross sectional anatomy, but didn't appear in the MRI images.

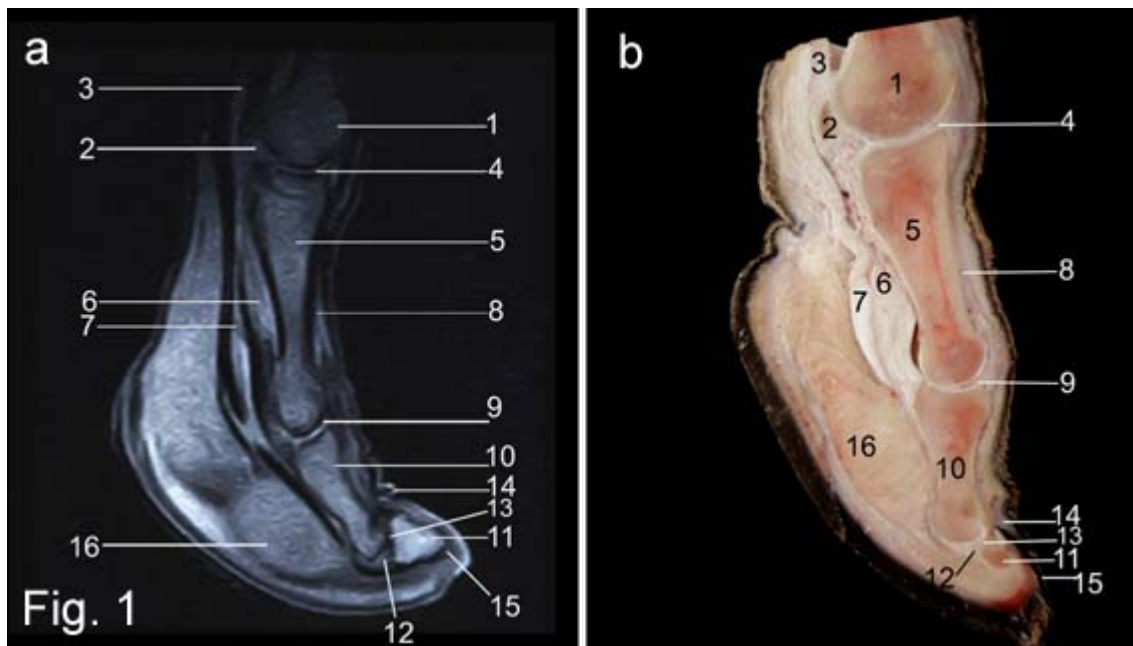


**Fig. 1: (a) Sagittal MRI image and (b) gross section of the left fore digits of the camel.**

1. Metacarpus IV; 2. Proximal sesamoid bone; 3. Interosseus medius muscle (sesamoid branch); 4. Metacarpophalangeal joint (fetlock joint); 5. Proximal phalanx; 6. Scutum medium; 7. Tendon of deep digital flexor muscle; 8. Common digital extensor tendon; 9. Proximal interphalangeal joint (Pastern joint); 10. Middle phalanx; 11. Distal phalanx; 12. Cartilaginous distal sesamoid; 13. Distal interphalangeal joint (Coffin joint); 14. Periople; 15. Nail; 16. Adipo-elastic digital cushion.

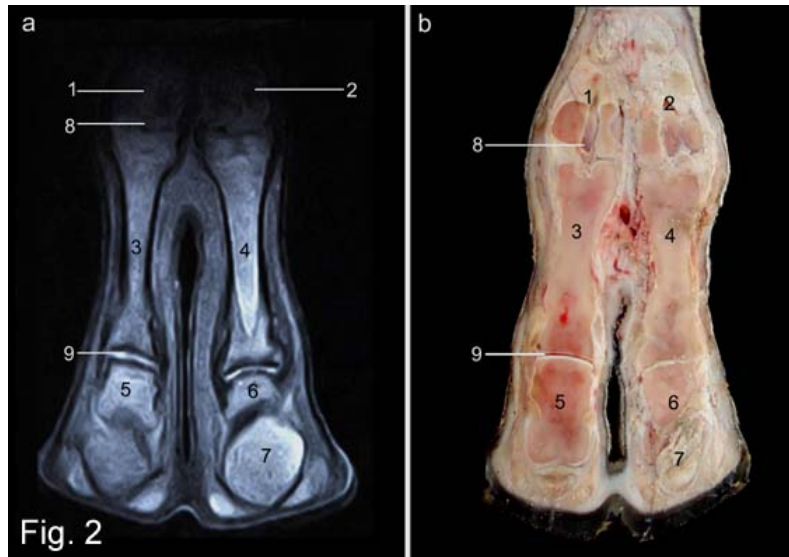


Fig. 2: (a) Dorsopalmar MRI image and (b) gross section of the left fore digits of the camel. 1. Metacarpus IV; 2. Metacarpus III; 3. Proximal phalanx of 4<sup>th</sup> digit; 4. Proximal phalanx of 3<sup>rd</sup> digit; 5. Middle digit of 4<sup>th</sup> digit; 6. middle phalanx of 3<sup>rd</sup> digit; 7. Adipo-elastic digital cushion; 8. Metacarpophalangeal joint (fetlock joint); 9. Proximal interphalangeal joint (Pastern joint).

The panel a of each following figures is a distal view of MRI scan and Panel b is a distal view of cross section.

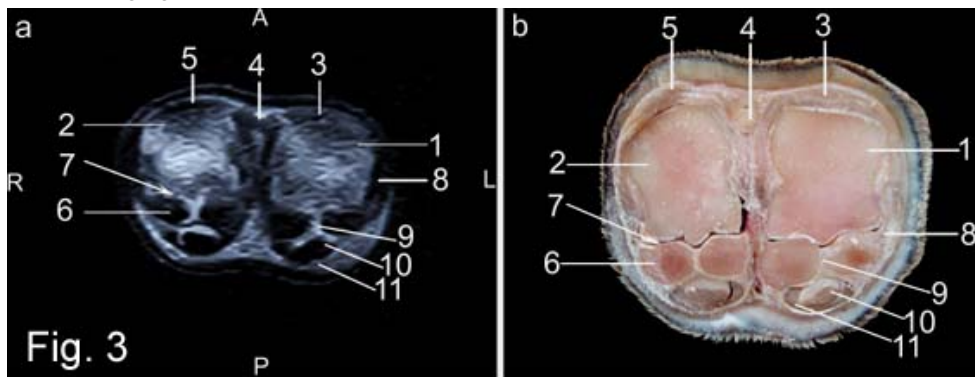


Fig.3: (a) Transverse MRI image and (b) cross- section of the left fore digits of the camel at the level of Metacarpophalangeal joint. 1. Distal end of the metacarpus IV; 2. Distal end of the metacarpus III; 3. Tendon of lateral digital extensor muscle; 4. True Common digital extensor tendon; 5. Medial tendon of common digital extensor muscle; 6. Proximal sesamoid bone; 7. Metacarpophalangeal articulation (Cavum articulare); 8. Collateral sesamoid Ligg; 9. Palmar ligg.; 10. Deep digital flexor tendon; 11. Superficial digital flexor tendon

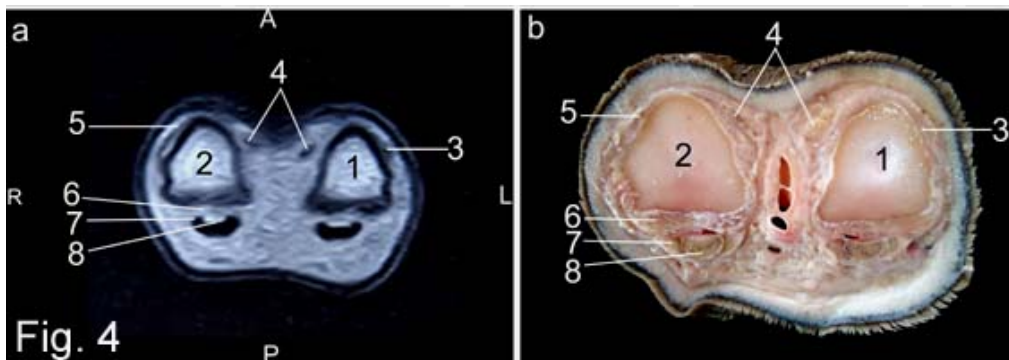


Fig. 4: (a) Transverse MRI image and (b) cross section of the left for digits of the camel at the level of the proximal end of the proximal phalanx.

1. Shaft of the proximal phalanx of digit IV; 2. Shaft of the proximal phalanx of digit III; 3. Tendon of lateral digital extensor muscle; 4. True Common digital extensor tendon( divided); 5. Medial tendon of common digital extensor muscle; 6. Interosseous muscle; 7. Superficial digital flexor tendon; 8. Deep digital flexor tendon.

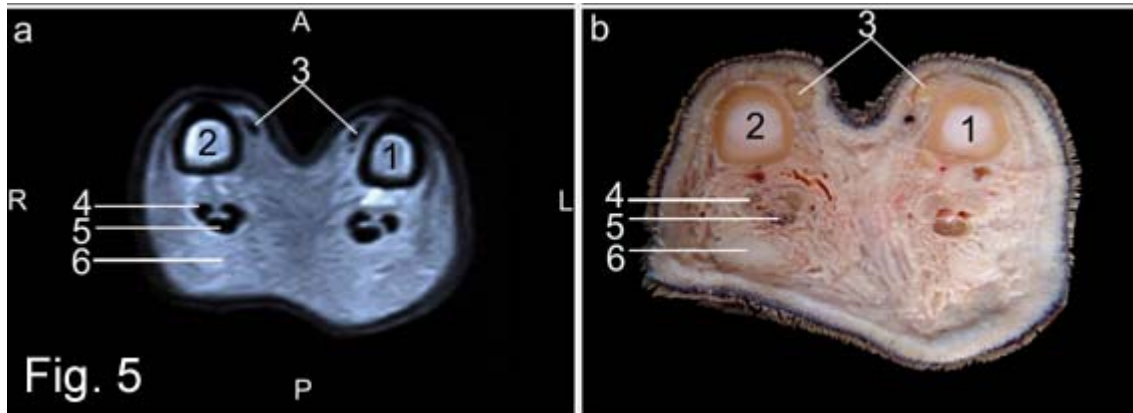


Fig. 5: (a) Transverse MRI image and (b) cross section of the left fore digits of the camel at the level of the middle of the body (shaft) of the proximal phalanx 1. Shaft of the proximal phalanx of digit IV; 2. Shaft of the proximal phalanx of digit III; 3. True common digital extensor tendon; 4. Superficial digital flexor tendon; 5. Deep digital flexor tendon; 6. Adipo-elastic digital cushion.

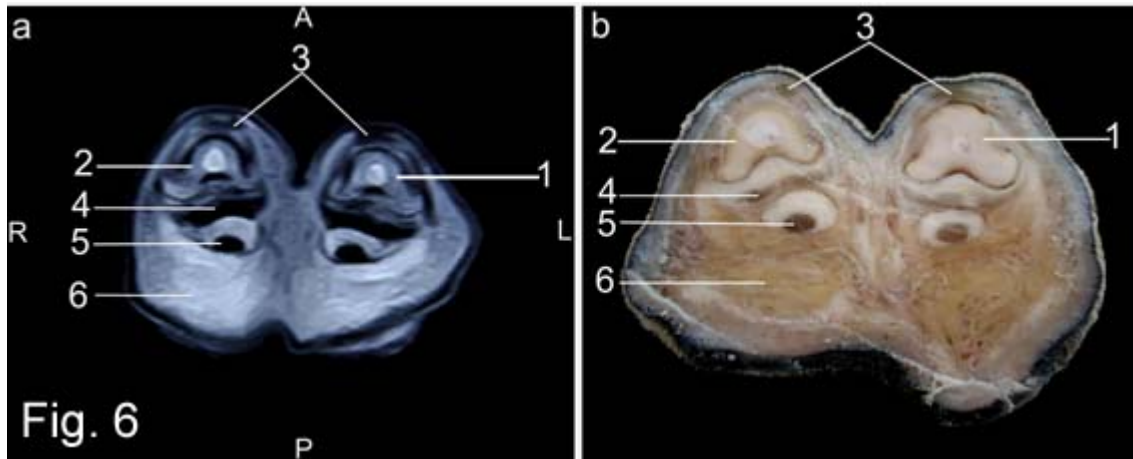


Fig. 6: (a) Transverse MRI image and (b) cross section of the left fore digits of the camel at the level of the distal end of the proximal phalanx. 1. Shaft of the proximal phalanx of digit IV; 2. Shaft of the proximal phalanx of digit III; 3. True common digital extensor tendon; 4. Superficial digital flexor tendon; 5. Deep digital flexor tendon; 6. Adipo-elastic digital cushion

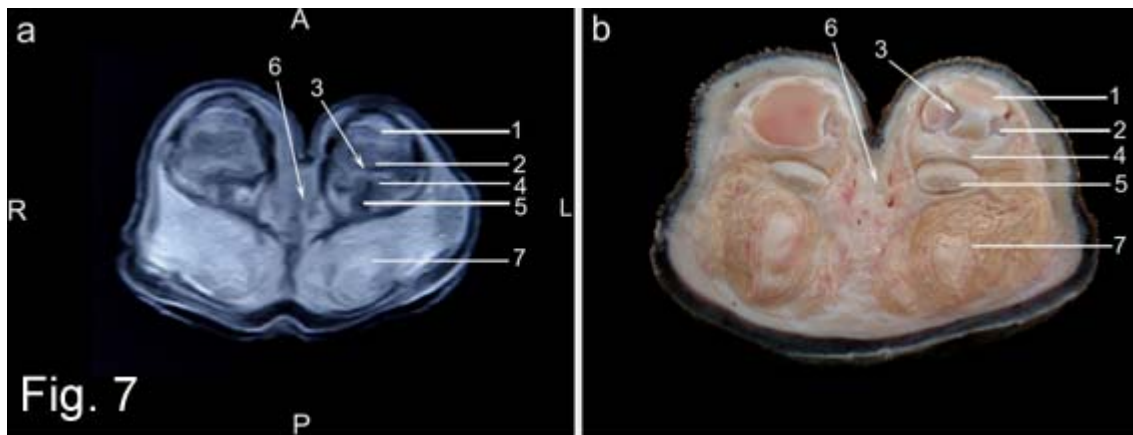


Fig.7: (a) Transverse MRI image and (b) cross section of the left fore digits of the camel at the level of the proximal interphalangeal (pastern) joint. 1. Distal end of the proximal phalanx of digit IV; 2. Proximal end of the middle phalanx of digit IV; 3. Proximal interphalangeal articulation (Cavum articulare); 4. Superficial digital flexor tendon; 5. Deep digital flexor tendon; 6. Interdigital lig; 7. Adipo-elastic digital cushion.

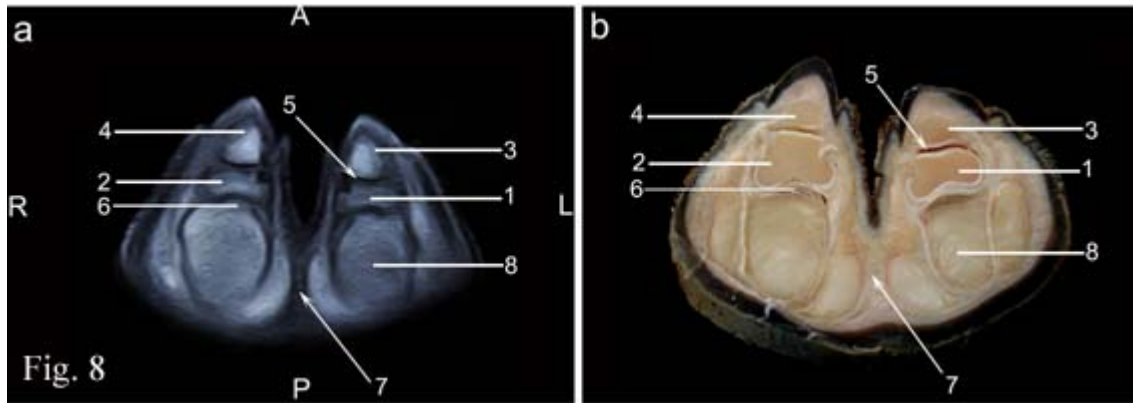


Fig 8: (a) Transverse MRI image and (b) cross section of the left fore digits of the camel at the level of the distal interphalangeal (Coffin) joint. 1. Middle phalanx of digit IV; 2. Middle phalanx of digit III; 3. Distal phalanx of digit IV; 4. Distal phalanx of digit III; 5. Distal interphalangeal articulation (Cavum articulare); 6. Deep digital flexor tendon; 7. Inter digital ligament; 8. Adipo-elastic digital cushion.

#### 4. Discussion

The present study stated the first information about the MRI scans of the digits of one humped camel. The present knowledge of normal cross sectional anatomy of the camel digits is essential for evaluation of MRI scans.

Advances in diagnostic techniques are continuously sought to assist clinical practitioners of veterinary medicine with making a definitive diagnosis, providing an accurate prognosis and determining the most appropriate treatment strategy. In the present study the MRI images of the camel digits provides acceptable details of the anatomical structures and were correlated well with its corresponding gross anatomical specimens. In accordance with Kleitoe *et al.*, 1999; Murray *et al.*, 2004; Hevesi *et al.*, 2004 and Dyson *et al.*, 2007, in horse, Raji *et al.*, 2009 in bovine' digits.

Foot and digits health and lameness are major issues facing dairy producers because of their common occurrence and the tremendous economic losses incurred (Shearer and Hernandez, 2000). Early detection and prompt treatment of the problem can minimize the loss, improve recovery, and reduce animal suffering (Shearer and Van Amstel, 2001).

MRI is based on the properties of certain elements, mainly hydrogen: to send a radiofrequency signal when it is under a magnetic field of a certain intensity stimulated by radio waves at an appropriate frequency. Advantages of MRI include Multiplan imaging, superior contrast resolution and (the absence of ionizing radiation (Shores, 1999). So, using MRI in camel research can open a window of opportunity for better understanding of the pathogenesis of some problems in camel such as laminitis and some other foot problems.

MRI can not only be used in diagnostic procedures but also can be used in many biometric research, measurements (Robina *et al.*, 1991 and Onar

*et al.*, 2002) and experimental (Paulus *et al.*, 2000, 2001). In all of these cases, a normal MRI image is necessary for identifying anatomical structure of the animal.

The use of MRI in camel 'medicine is partially limited because of expense the low availability of a suitable unit and a non-magnetic anesthetic unit. Nevertheless, these images should provide useful reference material for further future clinical studies of camel digits.

The present study serve as an initial reference aid in MRI imaging diagnosis of the one-humped camel digits disorders. More benefits could be harvested from MRI imaging when a future study is focused on certain part or joint, especially when the inter-slicing space is few millimeters.

#### Corresponding author

El-Shafey, A.A

Dept. Anat. & Embry, Fac. Vet. Med., Benha Univ. Egypt.

[Elshafey74@yahoo.com](mailto:Elshafey74@yahoo.com)

[Atef\\_abdalgali2005@yahoo.com](mailto:Atef_abdalgali2005@yahoo.com)

#### References

1. Assheuer, J. and M. Sager (1997): MRI and CT Atlas of the dog. 1<sup>st</sup> Ed. Blackwell Science. Berlin, Wien, Oxford.
2. Bahgat, H., 2007. Computed Tomography and Cross Sectional Anatomy of the Metacarpus and Digits of the Small Ruminants. Benha Vet. Med. J. 18, 63-84.
3. Bienert, A. and Stadler, P., 2006. Computed tomographic examination of the locomotor apparatus of horses a review. *Pferdeheilk.* 22, 218-226.

4. Denoix, J.M., N. Crevier, B. Roger and J.F. Lebas, 1993. Magnetic resonance imaging of the equine foot. *Veterinary Radiology and Ultrasound*, 6: 405-411.
5. Dyson, S., Murray, R., 2007. Magnetic Resonance Imaging of the Equine Foot. *Clin Tech Equine Pract.*, 6, 46-61.
6. Fahmy, L. S.; Farag, K. A.; Hegazy, A. A.; Zabady, M. K. 2002. Angular fetlock deformity of the fore limbs in camels: clinical, radiological and histopathological studies. *Scientific Journal of King Faisal University (Basic and Applied Sciences)* 2002 Vol. 1 No.(1): pp. En85-En100
7. Gehrmann, S., Hohne, K.H., Linhart, W., et al., 2006. A novel interactive anatomic atlas of the hand. *Clin. Anat.* 19, 258-66.
8. Goncalves-Ferreira, A.J., Herculano-carvalho, M., Melanica, J.P., Farias, J.P., Gomes, L., 2001. Corpus callosum: microsurgical anatomy and MRI. *Surgical Radiology & Anatomy*, 23:409-414.
9. Hevcsi, A., Stanek. C. H., Garamvolgyi, R., Petrasi, Z., Bongor, P., Repa, I., 2004. Comparison of the navicular region of newborn foals and adult horses by magnetic resonance imaging. *Journal Veterinary Medicine a.* 513:143-149.
10. Hundson, L.C., Cauzinille, I., Kornegay, J.N., Tompkins, M.B., 1995. Magnetic resonance imaging of the normal feline brain. *Veterinary Radiology & Ultrasound.* 36:267-275.
11. Janis, C.M., J.M Theodor and B. Biosvert, 2002. Locomotor evaluation in camels revisited: A quantitative analysis of pedal anatomy and the acquisition of the pacing gait. *J. Vertebrate Paleontol.*, 22(1): 110-121.
12. Kakhainen, M., Mero, M., Nummi, P., Pimto, L., 1991. Low field magnetic resonance imaging of the canine central nervous system. *Veterinary Radiology & Ultrasound*, 32:71-74.
13. Kazer-hotz. B.S., Sartoretto-Schefer, S., Weiss, R., 1994. Computed tomography and magnetic imaging of the normal equine carpus. *Veterinrv Radiology & Ultrasound*, 6:457-461.
14. Kleitoer. M., Kneissl, S., Stanek, G., Mayrhofer. F., Baulain. U., Deeger, E., 1999. Evaluation of Magnetic resonance imaging techniques in, the equine digit. *Veterinary Radiology & Ultrasound*, 401: 15-22.
15. Kraft. S.L., Gavin, P., Wedling, L. R., Reddy, V. K., 1986. Canine brain anatomy of magnetic resonance imaging. *Veterinary Radiology* 30:147-58.
16. Lisher, C.J. and U. Walliser, 2005. Fracture of the paracondylar process in four horses: advantages of CT imaging. *Equine Veterinary J.*, 37(5): 483-487.
17. Masahiko, M.T., Y. Tetsuya, K. So, B. Rai and H. Yoshihiro, 2002. Regional anatomy of the camel II. Comparison of the sole pads of the forelegs and hind legs of the two-humped camel (*Camelus bactrainus*). *Yamaguchi J. Veterinary Med.*, 29:11-18.
18. Morgan, R.V., Daneil, G.B., Donell, R.L., 1993. Magnetic resonance imaging of the normal eye and orbit of the dog and cat. *Veterinary Radiology & Ultrasound*, 35:102-108.
19. Murray, R.C., Dyson, S.J., Schramme. M.C., Branch, M., woods. S., 2004. Magnetic resonance imaging of the equine digit with chronic Laminitis. *Veterinary Radiology & Ultrasound*, 446:609-617.
20. Nickle, R., Schummer, A., Seiferle, E., 1995. *The anatomy of the domestic animals.* (Springer Erlag, Berlin and Hamburg), 2: 69-71, 428-432, 191-197.
21. Nomina Anatomica Veterinaria., 2005. 5<sup>th</sup> edition. Prepared by the international Committee on Veterinary Gross Anatomical Nomenclature (I.C.V.G.A.N) and authorized by the General Assembly of the World Association of Veterinary Anatomists (W.A.V.A.), Knoxville, TN (USA). Published by the Editorial Committee, Hannover, Columbia, Gent, Sapporo.
22. Onar, V., Kahvecioglu, K.O., Cebi, V., 2002. Computed tomography analysis the German shepherd dog (Alsatian) puppies. *Veterinary Arhiv*, 72:57-66.
23. Ottesen, N. and L. Moe, (1998): An introduction to computed tomography (CT) in the dog. *Eur. J. Compan. Anim. Pract.* 8, 29-36.
24. Paulus, M.J., Gleason, S.S., Eastery, M.E., Foils, C.J., 2001. A review of high resolution x-ray computed tomography and other imaging modalities for small animal research. *Laboratory Animal*, 30:36-45. Popesko, P., 1975. *Atlas of topographical anatomy of the domestic animals.* (WB Saunders. Philadelphia), 3:23-33, 61-65.
25. Paulus, M.J., Gleason, S.S., Kennel, S.J., Hun sicker, P.R., Johnson, D.K., 2000. High resolution x-ray. computed tomography: an emerging tool for small animal cancer research. *Neoplasia*, 2:6270.
26. Raji, A. R., Sardari. K., Mohammadi. H. R., 2008: Normal cross sectional anatomy of the bovine digit; Comparison of Computed Tomography and

- limb anatomy. *Anat. Histol. Embryol.*, 37:188-191.
27. Raji, A. R., Sardari. K., Mirmahmood. P., 2009. Magnetic resonance imaging of the normal bovine digit. *Vet Res Commun* 33:515-520.
  28. Robina, A., Regedon. S., Guillen. M.T., Lingnercux, Y., 1991: Utilization of computerized tomography for the determination of the volume of the cranial cavity of the Galgo Hound. *Acta Anatomica*, 140:108-111.
  29. Sampson SN, Schneider RK, Tucker RL, 2005: Magnetic resonance imaging of the equine distal limb, in Auer JA, Stick JA (eds): *Equine Surgery* (ed 3). Philadelphia, PA, Saunders, pp 946-963
  30. Sampson SN and Tucker RL, 2007: Magnetic Resonance Imaging of the Proximal Metacarpal and Metatarsal Regions. *Clin Tech Equine Pract* 6:78-85
  31. Schaller, O., 2007. *Illustrated Veterinary Anatomical Nomenclature* 2nd Edition. Enke Verlag. Stuttgart
  32. Shearer, J. K. and Hemanchez, J., 2000. Efficacy of two modified non-antibiotic formulations of (Victory TM) for treatment of papillomatous digital in dairy cows. *J Dairy Sci*, 83:741-745.
  33. Shearer. J.K. and Van Amstel. S. R., 2001. Functional and corrective claw trimming. *The veterinary clinics of North America, food animal practice*, 171:53-72.
  34. Shores, A., 1999. New and future advanced imaging techniques. *Veterinary Clinics of North American. Small Animal Practice*, 23:461-469.
  35. Smuts, M.S., Bezuidenhout, A.J., 1987. *Anatomy of the dromedary*. Clarendon Press, Oxford.
  36. Vanderperren, K., Ghaye, B., Hoegaerts, M., et al., 2008. Computed Tomographic Anatomy of the Equine Metacarpophalangeal Joint. *Vet. Radiol. & Ultrasound*. 49, 196–219.
  37. Webb, S.D., 1972. Locomotor evolution in camels. *Forma et Functio*, 5: 99-112.
  38. Zubrod CJ, Schneider RK, Tucker RL., 2004: Use of magnetic resonance imaging for identifying subchondral bone damage in horses: 11 cases (1999-2003). *J Am Vet Med Assoc.*, 224:411-418.

7/9/2012